Transient supramolecular hydrogels formed by catalytic control over molecular self-assembly

Wang, Hucheng; Liu, Liqun; Bai, Shengyu; Guo, Xuhong; Eelkema, Rienk; Van Esch, Jan H.; Wang, Yiming

DOI
10.1039/d0sm01584a

Publication date
2020

Document Version
Accepted author manuscript

Published in
Soft Matter

Citation (APA)
Wang, H., Liu, L., Bai, S., Guo, X., Eelkema, R., Van Esch, J. H., & Wang, Y. (2020). Transient supramolecular hydrogels formed by catalytic control over molecular self-assembly. *Soft Matter*, *16*(41), 9406-9409. https://doi.org/10.1039/d0sm01584a

Transient supramolecular hydrogels formed by catalytic control over molecular self-assembly

Hucheng Wang[†a], Liqun Liu[†a], Shengyu Bai[a], Xuhong Guo[a], Rienk Eelkema[b], Jan H. van Esch*[b] and Yiming Wang*[a]

The present work shows how transient supramolecular hydrogels can be formed by catalytically controlled molecular self-assembly. Catalysis formation of molecular gelators leads the self-assembly along a kinetically favored pathway resulting in transient hydrogels. This work demonstrates an effective approach towards pathway-dependent supramolecular materials.

Out-of-equilibrium self-assembly are widely observed in nature, contributing to the sophisticated functions of biological systems. Therefore, controlling self-assembly to proceed under out-of-equilibrium conditions may unlock new functions that are not associated with typical thermodynamic occasions, in that they can be autonomous,[1, 2] self-healing,[3, 4] adapting,[5, 6] or even self-replicating.[7-9] As such, the development of out-of-equilibrium self-assembly systems in manmade scenarios has been the focus of great interest in recent years.[10, 11] With the access to synthetic mimics, one can on the one hand get insight into the complex functions of biology, and, importantly, on the other hand design new synthetic materials with unparalleled functionalities.[12]

Towards out-of-equilibrium supramolecular structures, one typical approach is to regulate the self-assembly along a pathway that does not proceed towards the thermodynamic equilibrium state, ultimately giving rise to supramolecular architectures stabilized at a local energy minimum state.[13] The key to this goal is to interfere with the self-assembly kinetics of the building blocks, thereon to force the self-assembly along a kinetically preferred pathway rather than the thermodynamic one.[14] Along this line, significant efforts has been invested in recent years, and a few elegant strategies, including catalytic pathway selection,[15-18] seeded self-assembly,[19-22] and programmed pH feedback,[23-25] have been developed to control the pathway of molecular self-assembly, leading to different supramolecular products showing distinctly different material properties while still using the identical building blocks.[26-29] Despite of these progresses, the examples of pathway-dependent out-of-equilibrium self-assembly remains scarce, impeding further advances in the fundamental researches and the design of more advanced systems.

Here we report on transient supramolecular hydrogels that are formed by catalytic control over the self-assembly of molecular gelators. The self-assembly system involves hydrazone-based gelators decorated with non-ionic (**G**) and anionic (**G**$^-$) groups that are formed *in situ* from their precursor molecules, hydrazide (**H**) and aldehydes (**A** and **A**$^-$, respectively) (Fig. 1a). Previous work has demonstrated that these differently charged gelators can self-assemble into neutral fibers (**F**) and negatively charged fibers (**F**$^-$) through a kinetic self-sorting

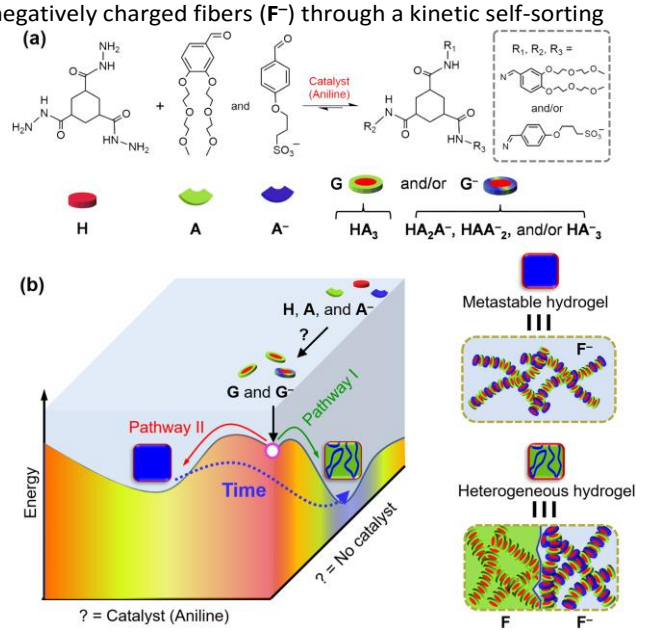

Fig. 1. a) Scheme of the formation of **G** (**HA$_3$**) and **G**$^-$ (**HA$_2$A**$^-$, **HAA**$^-_2$, and **HA**$^-_3$) from the building blocks of **H**, **A**, and **A**$^-$; b) self-assembly energy landscapes of **G** and **G**$^-$ along different pathways controlled by aniline catalysis.

process at the molecular level.[30] The resulting fibers can further organize into thermodynamically more stable heterogeneous hydrogels comprised **F**$^-$-rich crumpled sheets surrounded by **F**-rich coarse fibrous networks through a higher level self-sorting process at the fiber scale (Pathway I in Fig. 1b, Fig. S1, ESI).[21, 30] Now, here we show that aniline catalysis dramatically accelerates the formation and self-assembly of hydrazone gelators, thereby bypassing the multilevel self-sorting processes and giving rise to kinetically favored homogeneous hydrogels consisting of thin **F**$^-$ (Pathway II in Fig. 1b). Over time, these homogeneous hydrogels spontaneously convert into the thermodynamically more stable heterogeneous ones, indicating the out-of-equilibrium property (Fig. 1b).

The previous study has pointed out that the different nucleation rates of **G** and **G**$^-$ are responsible for the kinetic self-sorting process, leading to the thermodynamically more stable heterogeneous hydrogels.[30] Thus interfering with the nucleation of gelators may force their self-assembly along a kinetically favored pathway, giving rise to kinetic outcomes.[21] In our self-assembly system, using aniline catalysis can effectively facilitate the formation rate of the hydrazone-based gelators,[18] thereby affecting the supersaturation and in turn the nucleation

of gelators. In this context, here we propose to use aniline catalysis to control self-assembly kinetics of the gelators with the aim to alter the self-assembly pathway and control the formation of out-of-equilibrium product.

We first employed oscillatory rheology to test the effects of aniline on the hydrogel formation (Fig. S2, ESI). All the samples were prepared using 0.1 M, pH 7.0 phosphate buffer, and the concentration of aldehyde (**A** + **A**$^-$) was constantly kept at six times higher than **H** to ensure a complete conversion of **H** into gelators.[18, 31] The results showed that the presence of aniline can significantly accelerate the gelation process (Fig. S2, ESI). For instance, for the sample prepared with 30 mol% **A**$^-$, the gelation time (the time when the elastic modulus G' starts to exceed the viscous modulus G'') was reduced from ~2.6 to ~0.25 h upon increasing the concentration of aniline from 0 to 15 mM (Fig. 2a). A remarkable drop in gelation time was observed as well in the other samples prepared with different contents of **A**$^-$ (Fig. 2a). Additionally, the stiffness of the resulting hydrogels was dramatically increased with the concentration of aniline (Fig. 2b). The plateau elastic modulus, G'_0, was enhanced from ~0.04 to ~4.5kPa for the sample containing 30 mol% **A**$^-$ or from ~0.70 to ~100.0 kPa for the sample containing 0 mol% **A**$^-$, upon

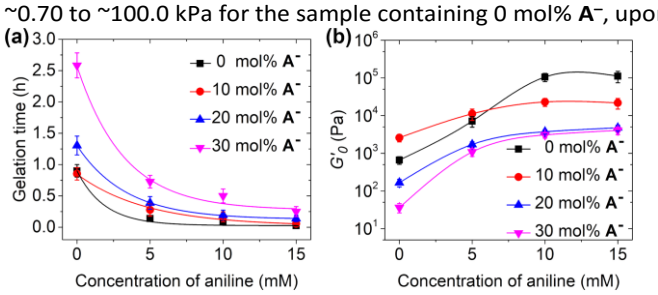

Fig. 2. Catalytic effects of aniline on the formation of hydrogels: a) gelation time; and b) hydrogel stiffness as a function of aniline concentrations. Samples: [**H**] = 20 mM, [**A** + **A**$^-$] = 120 mM (different mol% **A**$^-$) in 0.1 M, pH 7.0 phosphate buffer. Error bars are the s.d. calculated from three independent measurements.

increasing aniline from 0 to 15 mM (Fig. 2b). The accelerated gelation process and increased hydrogel stiffness are attributed to the rapid formation of gelators catalyzed by aniline, which has been demonstrated in a previous study.[18] Moreover, we further found that the presence of aniline substantially decreased the critical concentration of **H** required for occurrence of gelation (CGC, Fig. S3, ESI), further showing the catalytic effects of aniline on the self-assembly of gelators.[18, 32] It is noteworthy that **A** and **A**$^-$ show identical reactivity with **H**,[30] thus the accelerated gelation results from the aniline catalysis rather than the composition variation of gelators. It is noteworthy that the pH of samples can be well buffered in the presence of aniline. These results suggest that hydrazone gelators are rapidly formed to reach a supersaturated state under aniline catalysis, thereby accelerating the nucleation of gelators and in turn resulting in the faster gelation.

After confirming the acceleration of aniline catalysis on the gelation process, we were keen to know the effects of catalysis on the morphologies of the resulting hydrogel networks. To study this effect, confocal laser scanning microscopy (CLSM) measurements were performed. Hydrogel samples prepared with different concentrations of aniline were labelled by aldehyde tailored fluorescein (**A-FL**) which is covalently linked to the fibers; moreover, cationic **Hoechst 33342** was used to identify the **F**$^-$ in the hydrogel networks on the basis of electrostatic interactions (Fig. S4, ESI).

We found that upon increasing the concentration of aniline from 0 to 15 mM, the networks of the hydrogels prepared with 0 mol% **A**$^-$ changed from large clusters to dense fibrous bundles (Fig. 3), in line with the previous study.[18] For the hydrogel samples prepared with **A**$^-$ (10 to 30 mol%), heterogeneous networks comprising **F**$^-$-rich crumpled sheets with **F**-rich bundling networks in between were formed in the absence of aniline (Fig. 3), which have been systematically investigated previously.[30] However, with increasing the concentration of aniline from 0 to 15 mM, the crumpled sheet structures gradually vanished, and instead, relatively more homogeneous networks are generated; when the concentration of aniline was increased to be higher than 10 mM, completely homogeneous fluorescence without any visible fibrous structures was observed (Fig. 3). Moreover, the transparency of the resulting hydrogel samples increased with the concentration of aniline (Fig. S5, ESI), which is in good agreement with the observed structural variations. The hydrogel turned complete transparent when made using 30 mol% **A**$^-$. Cryo-TEM measurements demonstrated that the homogeneous hydrogel networks were mainly composed of single nanofibers with a diameter of ~5.8 nm (Fig. S6, ESI), in keeping with the homogeneity of the hydrogel networks observed in CLSM tests. Furthermore, cationic **Hoechst 33342** showed that the thin fibers in the homogeneous hydrogel networks were **F**$^-$ (Fig. S7, ESI). The evolution from large clusters to dense fibers with addition of aniline would lead more fibers to participate in the crosslinking of hydrogel networks, explaining the high gel stiffness and low CGC as discussed above.

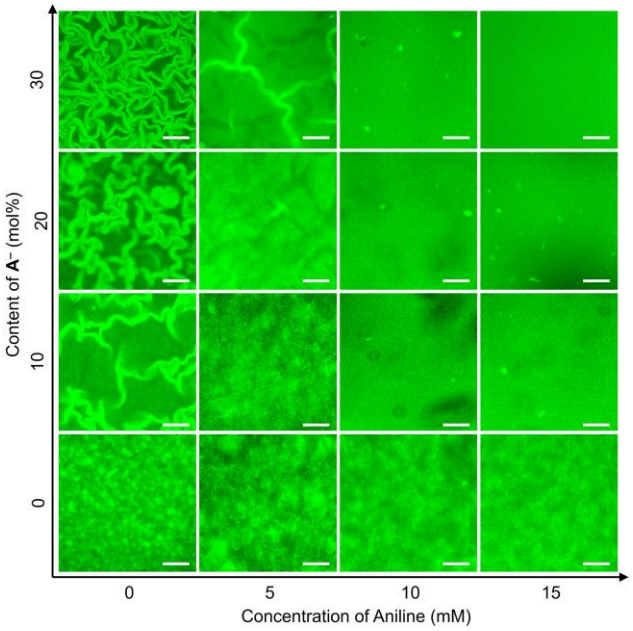

Fig. 3. CLSM images showing the morphology variations of the hydrogel networks against the concentration of aniline and the content of **A**$^-$. Samples: [**H**] = 20 mM, [**A** + **A**$^-$] = 120 mM

(different mol% **A**$^-$), [**A-FL**] = 30 μM in 0.1 M, pH 7.0 phosphate buffer. Scale bars = 40 μm.

These morphological characterization results together with the rheological results strongly suggest that the rapid formation of **G** and **G**$^-$under the aniline catalysis leads to a high supersaturation level, which dramatically accelerates the nucleation of gelators, leading to co-assembly instead of self-sorting of **G** and **G**$^-$. As a result, only **F**$^-$ is formed, giving rise to formation of the kinetically favored homogeneous hydrogel networks. The electrostatic repulsions between **F**$^-$ effectively prevent the occurrence of bundling, explaining the low dimension of the fibrous networks as observed in CLSM tests.

The preceding investigations clearly demonstrate that using of aniline catalysis forces the self-assembly of **G** and **G**$^-$ along a kinetically controlled pathway, giving rise to kinetically favored homogenous hydrogels (Fig. 4a). To examine the out-of-equilibrium properties of these kinetic hydrogels, we incubated the hydrogel samples against time under ambient conditions. Interestingly, after a storage of the hydrogel samples for ~16 days, we found that the crumpled sheet structures with small visible clusters in between were formed in the hydrogel networks, showing comparable morphologies to the thermodynamically more stable heterogeneous hydrogels (Fig. 4b). Cryo-TEM measurements confirmed that the 16-day aged hydrogels were composed of thin single fibers and large fibrous bundles (Fig. 4c). Furthermore, upon addition of **Hoechst 33342**, we identified that the crumpled structures were mainly composed of **F**$^-$, while the small clusters in between mainly consisted of **F** (Fig. S8, ESI). Thus it can be concluded from these results that, through aniline catalysis, homogeneous kinetic hydrogels composed of **F**$^-$ are transiently formed and are capable of converting into the thermodynamically more stable heterogeneous hydrogels over time.

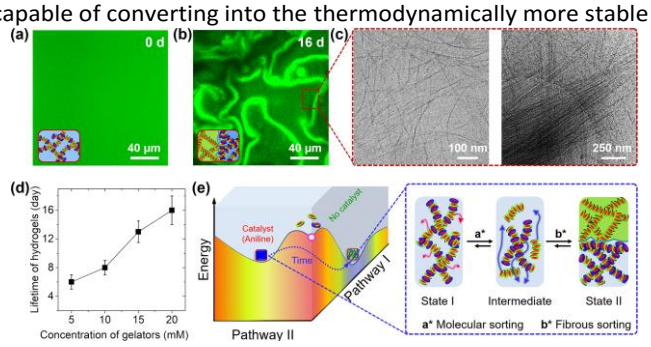

Fig. 4. a, b) CLSM images of a) freshly prepared and b) 16-day aged kinetic hydrogel; c) cryo-TEM images of the 16-day aged kinetic hydrogel; d) lifetime of the kinetic hydrogels against gelator concentration, the error bars are s.d. of the measurements of three parallel samples; and e) illustration of the time-dependent evolution process of the kinetic hydrogel networks. The hydrogel samples in a-c): [**H**] = 20 mM, [**A** + **A**$^-$] = 120 mM (30 mol% **A**$^-$), [**A-FL**] = 30 μM, [aniline] = 15 mM in 0.1 M, pH 7.0 phosphate buffer; and in d): [**H**]/[**A** + **A**$^-$] = 1/6 (30 mol% **A**$^-$), [Aniline] = 15 mM in 0.1 M, pH 7.0 phosphate buffer.

To further insight into the structural evolution process, we measured the lifetime of the hydrogels against the concentration of gelators using CLSM, where the lifetime was defined as the time when the heterogeneous hydrogel networks starts to be observed (Fig. S9, see supporting information). All the tested hydrogel samples were prepared with addition of 15 mM aniline to ensure efficient catalysis. It was found that the lifetime of the resulting hydrogels was increased from ~6 to ~16 days with increasing the concentration of gelators from 5 to 20 mM (Fig. 4d). The increase of lifetime with concentration of gelators indicates that the homogeneous kinetic hydrogels are off-pathway or competitive pathway outcomes in respect to the thermodynamic state according to previous studies;[14, 33] and during the structural transformation, gelators **G** and **G**$^-$ first escape the **F**$^-$ in homogeneous kinetic hydrogels and then reassemble into **F** and **F**$^-$ through a molecular self-sorting process (**a*** step in Fig. 4e),[34] which further organize into heterogeneous hydrogels through fiber self-sorting as demonstrated before (**b*** step in Fig. 4e).[30]

Conclusions

In summary, we have demonstrated how transient supramolecular hydrogels can be prepared through catalytic control over self-assembly of molecular gelators. In a hydrazone-based modular gelator system, the formation of gelators is dramatically accelerated to rapidly reach a supersaturated level, facilitating the nucleation of gelators. Thereon, the presence of catalysis forces the self-assembly of gelators along a kinetically favored pathway, giving rise to hydrogel products showing very different network morphologies and mechanical properties from the thermodynamically more stable ones. Interestingly, these kinetically more preferred hydrogels show finite lifetime, and are capable of transforming into the thermodynamically more stable states over time. Furthermore, we have unveiled that the formation of these kinetically favored transient hydrogels are associated with an off-pathway or competitive pathway self-assembly in respect to the thermodynamic self-assembly. Such catalytic control over molecular self-assembly leading to transient supramolecular structures can serve as a useful alternative way towards out-of-equilibrium supramolecular materials with pathway-dependent properties for high-tech applications.[35, 36]

Conflicts of interest

There are no conflicts to declare.

Acknowledgements

We thank Dr. J. M. Poolman and Dr. C. Maity for synthesis of **H**, **A**, **A**$^-$, and **A-FL**. We would like to acknowledge the NSFC Grants (21908061), the Fundamental Research Funds for the Central Universities (JKA012016012) and the ECUST Innovation Program (SP2002A001) for financial support.

Notes and references

1 G. Ragazzon, M. Baroncini, S. Silvi, M. Venturi and A. Credi, *Nat. Nanotechnol.*, 2015, **10**, 70.
2 M. Nijemeisland, L. K. E. A. Abdelmohsen, W. T. S. Huck, D. A. Wilson and J. C. M. van Hest, *ACS Central Sci.*, 2016, **2**, 843.
3 K. D. Birnbaum and A. Sanchez Alvarado, *Cell*, 2008, **132**, 697.
4 F. J. Nedelec, T. Surrey, A. C. Maggs and S. Leibler, *Nature*, 1997, **389**, 305.
5 J. D. Halley and D. A. Winkler, *Complexity*, 2008, **14**, 10.
6 R. Weinkamer, J. W. C. Dunlop, Y. Brechet and P. Fratzl, *Acta Mater.*, 2013, **61**, 880.
7 J. M. A. Carnall, C. A. Waudby, A. M. Belenguer, M. C. A. Stuart, J. J. P. Peyralans and S. Otto, *Science*, 2010, **327**, 1502.
8 K. Kurihara, M. Tamura, K. Shohda, T. Toyota, K. Suzuki and T. Sugawara, *Nat. Chem.*, 2011, **3**, 775.
9 J. W. Sadownik, E. Mattia, P. Nowak and S. Otto, *Nat. Chem.*, 2016, **8**, 264.
10 J. H. van Esch, R. Klajn and S. Otto, *Chem. Soc. Rev.*, 2017, **46**, 5474.
11 B. Riess, R. K. Grotsch and J. Boekhoven, *Chem*, 2020, **6**, 552.
12 R. Merindol and A. Walther, *Chem. Soc. Rev.*, 2017, **46**, 5588.
13 A. Sorrenti, J. Leira-Iglesias, A. J. Markvoort, T. F. A. de Greef and T. M. Hermans, *Chem. Soc. Rev.*, 2017, **46**, 5476.
14 P. A. Korevaar, S. J. George, A. J. Markvoort, M. M. Smulders, P. A. Hilbers, A. P. Schenning, T. F. De Greef and E. W. Meijer, *Nature*, 2012, **481**, 492.
15 C. G. Pappas, I. R. Sasselli and R. V. Ulijn, *Angew. Chem. Int. Ed.*, 2015, **54**, 8119.
16 S. Debnath, S. Roy and R. V. Ulijn, *J. Am. Chem. Soc.*, 2013, **135**, 16789.
17 J. K. Sahoo, C. G. Pappas, I. R. Sasselli, Y. M. Abul-Haija and R. V. Ulijn, *Angew. Chem. Int. Ed.*, 2017, **56**, 6828.
18 J. Boekhoven, J. M. Poolman, C. Maity, F. Li, L. van der Mee, C. B. Minkenberg, E. Mendes, J. H. van Esch and R. Eelkema, *Nat. Chem.*, 2013, **5**, 433.
19 T. Fukui, S. Kawai, S. Fujinuma, Y. Matsushita, T. Yasuda, T. Sakurai, S. Seki, M. Takeuchi and K. Sugiyasu, *Nat. Chem.*, 2017, **9**, 493.
20 T. Fukui, M. Takeuchi and K. Sugiyasu, *Sci. Rep.*, 2017, **7**, 2425.
21 Y. Wang, R. M. de Kruijff, M. Lovrak, X. Guo, R. Eelkema and J. H. van Esch, *Angew. Chem. Int. Ed.*, 2019, **58**, 3800.
22 Y. M. Wang, T. K. Piskorz, M. Lovrak, E. Mendes, X. H. Guo, R. Eelkema and J. H. van Esch, *Adv. Sci.*, 2020, **7**, 1902487.
23 T. Heuser, E. Weyandt and A. Walther, *Angew. Chem. Int. Ed.*, 2015, **54**, 13258.
24 T. Heuser, A. K. Steppert, C. M. Lopez, B. L. Zhu and A. Walther, *Nano Lett.*, 2015, **15**, 2213.
25 S. Panja, C. Patterson and D. J. Adams, *Macromol. Rapid Commun.*, 2019, **40**.
26 S. Ogi, T. Fukui, M. L. Jue, M. Takeuchi and K. Sugiyasu, *Angew. Chem. Int. Ed.*, 2014, **53**, 14363.
27 E. E. Greciano, B. Matarranz and L. Sanchez, *Angew. Chem. Int. Ed.*, 2018, **57**, 4697.
28 A. M. Fuentes-Caparros, F. D. Gomez-Franco, B. Dietrich, C. Wilson, C. Brasnett, A. Seddon and D. J. Adams, *Nanoscale*, 2019, **11**, 3275.
29 S. Panja, K. Boháčová, B. Dietrich and D. J. Adams, *Nanoscale*, 2020, **12**, 12840.
30 Y. Wang, M. Lovrak, Q. Liu, C. Maity, V. A. A. le Sage, X. Guo, R. Eelkema and J. H. van Esch, *J. Am. Chem. Soc.*, 2019, **141**, 2847.
31 J. M. Poolman, J. Boekhoven, A. Besselink, A. G. Olive, J. H. van Esch and R. Eelkema, *Nat. Protoc.*, 2014, **9**, 977.
32 R. Eelkema and J. H. van Esch, *Org. Biomol. Chem.*, 2014, **12**, 6292.
33 S. Ogi, K. Sugiyasu, S. Manna, S. Samitsu and M. Takeuchi, *Nat. Chem.*, 2014, **6**, 188.
34. J. Matern, Y. Dorca, L. Sanchez and G. Fernandez, *Angew. Chem. Int. Ed.*, 2019, **58**, 16730.
35. W. Ji, G. Liu, Z. Li, and C. Feng, *ACS Appl. Mater. Interfaces*, 2016, **8**, 5188.
36. L. Yang, J. Huang, M. Qin, X. Ma, X. Dou and C. Feng, *Nanoscale*, 2020, **12**, 6233.